Chapter 1

Introduction

Liquid crystals are the states of matter, which have the properties of liquids as well as crystals. Certain organic materials, on heating, do not just show a single transition from crystal to liquid, but rather a series of transitions involving intermediate phases. The mechanical, optical and symmetry properties of these phases are intermediate between those of a liquid and those of a crystal. These intermediate phases are known as *Liquid Crystalline* phases. A more appropriate name for them is *Mesomorphic Phases* (mesomorphic: of intermediate form). Liquid crystalline properties are exhibited by several different systems. In addition to certain types of organic systems, micellar solution of surfactants, main and side chain polymers and a large number of biological systems are known to have liquid crystalline properties [1].

This thesis deals with the optical properties of some liquid crystalline systems. In this chapter we give a brief overview of liquid crystals and then we discuss about dynamic light scattering (DLS). We also give a description of the nonlinear optical properties of liquid crystals.

1.1 An overview of liquid crystals

Liquid crystalline phases possess the properties characteristic of both the crystals and liquids like elasticity, viscosity and surface tension. Even within the liquid crystalline phases there may be various types of ordering leading to different liquid crystalline sub phases.

Liquid crystals are divided into two categories, namely, *Thermotropic liquid crystals* and

Lyotropic liquid crystals depending on the phase inducing factors.

- **Thermotropic liquid crystals:** In these liquid crystals, the phase transitions can be brought about by changing the temperature of the system [1, 2]. A vast majority of liquid crystalline compounds fall in this category. Thermotropic liquid crystals have gained a lot of attention in the recent times because of their practical importance in display technology.

- **Lyotropic liquid crystals:** This class of liquid crystals comprising multicomponent systems also show a rich variety of phases [3]. Lyotropic liquid crystalline phases are shown by amphiphilic molecules (have a hydrophilic and hydrophobic part) dissolved above a certain concentration in a solvent which is usually water. The liquid crystals phase transitions are brought about by changing the relative concentration of various components or sometimes temperature. Lyotropic liquid crystals are also extremely important because of their role in biological membranes. Membranes are composed of amphiphilic lipids - mostly phospholipids and cholesterol, with a small percentage of glycolipids. These liquid crystals also find useful applications in soap industries. In the medical applications, a lyotropic liquid crystal can be used to coat a drug which prevents it from being destroyed in the digestive tract. The drug can then be taken orally and after it reaches the proper location in the body, the drug can be released by breaking down the liquid crystalline phase.

In the following subsections, we introduce some of the main features of commonly occurring liquid crystal phases such as, nematics, cholesterics and smectics.

1.1.1 The nematic phase

The word “nematic” comes from the Greek $\nu\eta\mu\alpha$ = *thread*. It refers to certain thread like defects which are commonly observed under the optical microscope in these materials. Nematics are the simplest liquid crystals. In this phase, the molecules have long range orientational ordering but there is no positional order.

In the nematic phase of rod-shaped molecules, the long axis of molecules point, on an average, along a particular direction in space as shown in Fig. 1.1. In nematic phase of disk like micelles[1] of amphiphilic molecules dissolved in water, the disks (see Fig. 1.2(a)) are arranged, on an average, perpendicular to a direction in space. This is shown in Fig. 1.2(b). A unit vector **n** is defined in this direction and is called as *director*. The probability of finding a molecule (or axis of the disk) parallel and anti parallel to the director is the same. This leads to the physical equivalence of **n** and $-\mathbf{n}$. The nematic phase is cylindrically symmetric about the director. The degree of orientational order of the molecules or disks in the nematic phase is defined by an order parameter S. The order parameter is defined as:

$$S = \frac{1}{2}\langle 3\cos^2(\theta_i) - 1\rangle \tag{1.1}$$

where, θ_i is the angle made by the i^{th} molecule (or axis of the disk) with the director and the angular brackets indicate a spatial average. The order parameter is a function of temperature and its typical value is about 0.4 in a nematic phase.

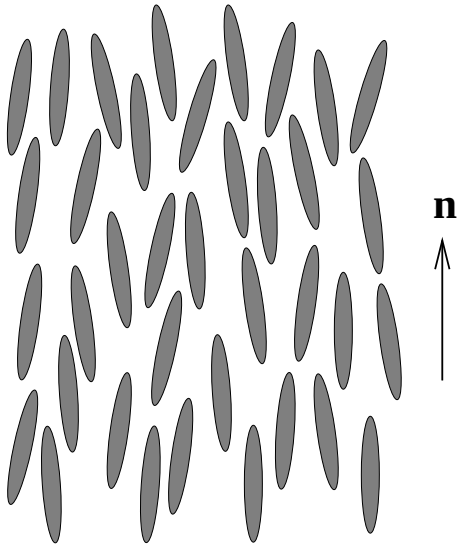

Figure 1.1: A schematic diagram of rod like molecules arranged in a nematic phase. The unit vector along the average direction of molecules is known as director (**n**).

The easiest way to identify whether a given compound shows a liquid crystalline phase

[1] A submicroscopic aggregation of molecules in a solvent. Micelles could be spherical, cylindrical or disk shaped.

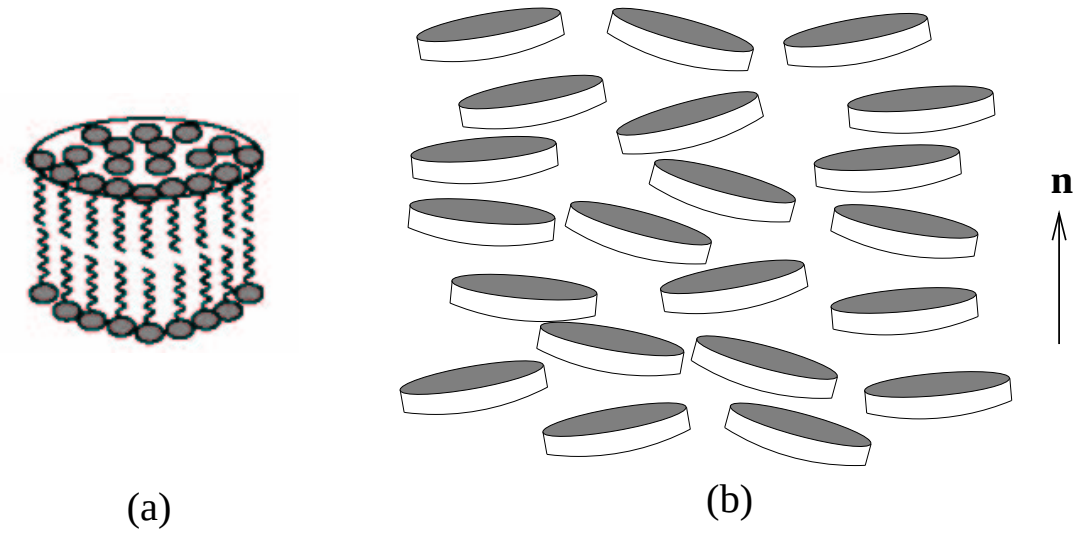

Figure 1.2: A schematic diagram of (a) disk like micelle of amphiphilic molecules dissolved in water and (b) these micelles arranged in a nematic phase.

or not is to see it under a polarizing microscope. A polarizing microscope is an ordinary optical microscope with an attached polarizer and an analyzer. A liquid crystal sample placed between the polarizer and analyzer (crossed with each other) of the polarizing microscope shows the textures characteristic of each type of liquid crystal. A nematic liquid crystal shows distinguished two brush and four brush defects (known as Schlieren texture [4]) under a polarizing microscope.

1.1.2 The cholesteric phase

A cholesteric (or chiral nematic) liquid crystal phase is shown by molecules which are either chiral[2] in nature or doped in small quantities with chiral molecules. The structure of a cholesteric liquid crystal is shown in Fig. 1.3. It consists of molecules in a statistically parallel arrangement of the director **n** just like the nematic phase. However, the asymmetry of the constituent molecules causes a slight and gradual spontaneous rotation of the director. The director describes a helix with a specific temperature dependent pitch. If we consider the z axis along the twist axis and the director in $x-y$ plane, then the cholesteric can be described

[2] An object or molecule that is not superimposable on its mirror image is known as chiral (Greek for handed).

by the following components:

$$n_x = \cos(q_0 z) \tag{1.2}$$

$$n_y = \sin(q_0 z) \tag{1.3}$$

$$n_z = 0 \tag{1.4}$$

where, $q_0 (= 2\pi/P)$ is the magnitude of the wave vector and P is the pitch of the helix. A cholesteric liquid crystal exhibits many beautiful optical properties like selective reflection of circularly polarized light and high optical rotation of a plane polarized light. This makes cholesterics useful commercial materials. The typical texture that a cholesteric phase exhibits under a polarizing microscope is *finger print* texture. This texture is observed with a large pitch cholesteric having the helix axis in the plane of the plates. This texture is very useful for directly measuring the pitch of a cholesteric. Low pitch cholesteric liquid crystal shows a *focal conic* texture which is also the characteristic of smectic A liquid crystals. A cholesteric liquid crystal also shows network like defect lines commonly known as *oily streaks* [4].

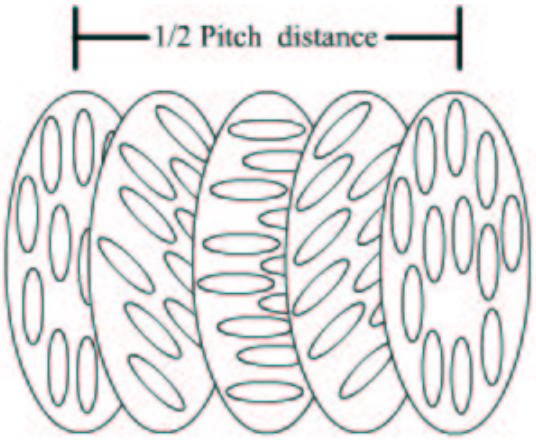

Figure 1.3: A schematic diagram of rod like molecules showing a cholesteric liquid crystal phase.

1.1.3 The smectic phase

Smectic (Greek $\alpha\mu\eta\gamma\mu\alpha$ = soap), refers to certain mesophases which have some mechanical properties like soaps. All the smectics are layered structures with a specific interlayer spac-

ing. The smectic phases are more ordered than nematics and hence generally, smectic phases occur at temperatures below the nematic phase. There exist different types of smectics, giving rise to different textures in polarizing microscope. Here, we describe a few of them.

Smectic A: Molecular arrangement of smectic A mesophase is shown in Fig. 1.4. The molecules are arranged in layers and within each layer there is no positional correlation. The system is optically uniaxial and optic axis is normal to the plane of layers. In a polarizing microscope, smectic A shows a *focal conic texture* and *fan texture* [4].

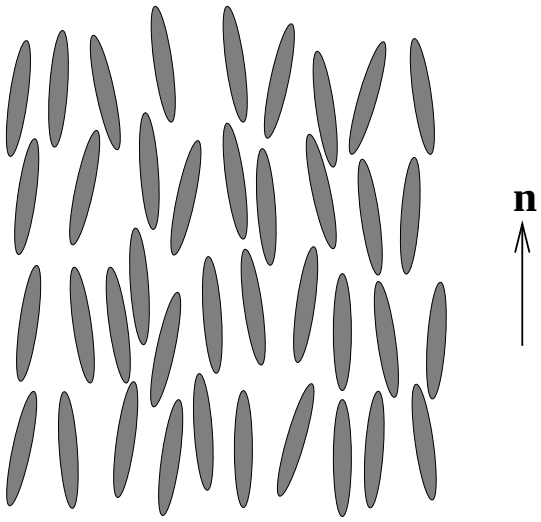

Figure 1.4: The rod like molecules arranged in layers in a smectic A phase. Layer normal is along the direction of the optic axis. Here, **n** represents the director.

Smectic C: Smectic C mesophase has a structure similar to that of smectic A except for the fact that the molecules in all the layers are uniformly tilted with respect to the layer normal. Each layer is a two dimensional fluid since there is no positional correlation within the layer. The molecular arrangement of smectic C mesophase is depicted in Fig. 1.5. The projection of director (**n**) along the layer is called **c** director. The **c** director is like the nematic director and therefore, a smectic C sometimes shows a Schlieren texture with only four brushes. Smectic C also shows focal conic texture because of the layered structure [4].

Chiral smectic C or Smectic C*: The smectic C structure is obtained only when the constituent molecules are optically inactive. If the molecules are intrinsically chiral or if we

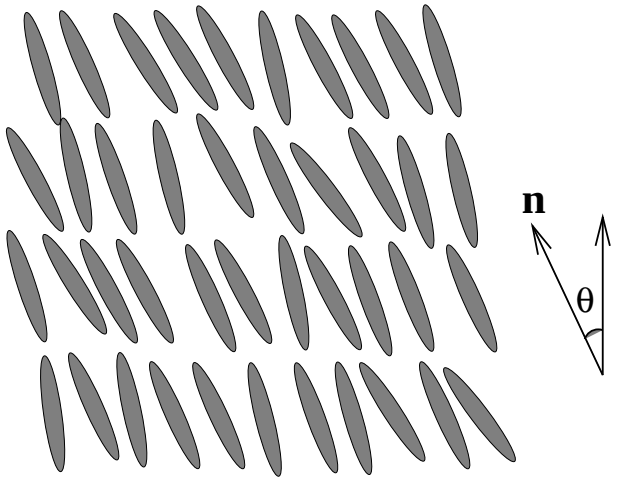

Figure 1.5: A schematic representation of a smectic C phase. The molecules are tilted with respect to the layer normal at an angle θ.

add the optically active (chiral) molecules to a smectic C, the structure gets modified. The direction of tilt precesses around the layer normal resulting in a helical configuration. This configuration is called chiral smectic C or smectic C*. Introducing chirality suppresses the symmetry and this leads to the fact that smectic C*s are ferroelectric. They show focal conic or Schlieren textures under a polarizing microscope [4]. It is difficult to identify smectic C* by using just a polarizing microscope, so definitive characterization of this phase is done by using x-ray diffraction.

Lamellar: There is another smectic liquid crystalline phase shown by amphiphilic molecules dissolved in water in appropriate concentration. This is known as *Lamellar phase* (neat soap phase), wherein extended sheets of amphiphilic molecules are separated by thin layers of water. A schematic of amphiphilic molecules arranged in lamellar phase is shown in Fig. 1.6.

There are also some disk like and bent core organic molecules which show liquid crystalline phases known as discotic and banana liquid crystals, respectively. Apart from these, there are also some other thermotropic and lyotropic phases like twist grain boundary (TGB), blue phases, cylindrical micellar, hexagonal columnar and inverse micellar phases. The TGB phase occurs between smectic and cholesteric phases and consists of a helical arrangement of

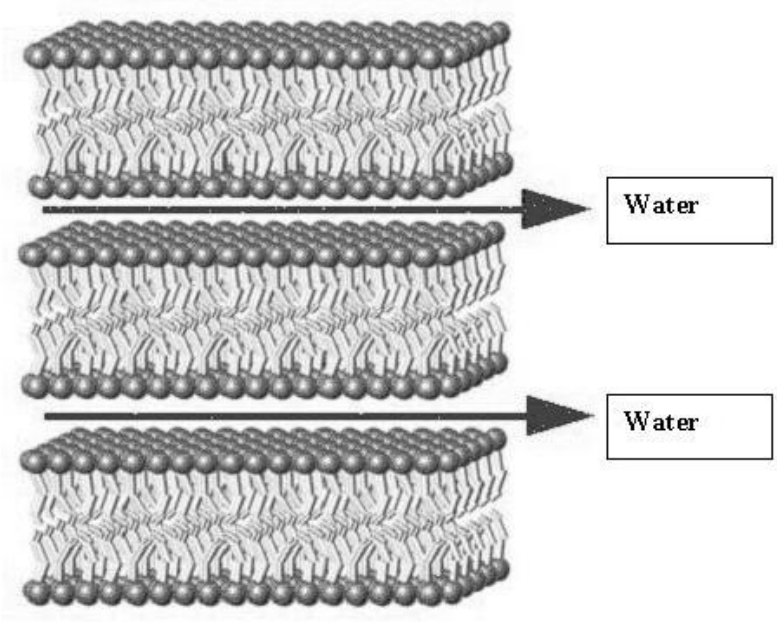

Figure 1.6: A schematic representation of lamellar phase. The amphiphilic molecules are arranged in bilayers.

smectic blocks separated by a twisted region made up of linear array of screw dislocations. The blue phases occur over a short range of temperatures near the cholesteric to isotropic transition.

1.2 Static distortion in the director

In this section we describe some mechanical properties of liquid crystal phases. Liquid crystalline molecules have high shape anisotropy which reflects in the bulk material properties like refractive index, magnetic susceptibility, dielectric constant and elastic constants. The clear difference in the mechanical properties like viscosity and elasticity of a liquid crystal and isotropic liquid is very striking. An isotropic fluid flows in all directions with same viscosity coefficient but in liquid crystals, the viscosity depends on the coupling of director to the flow field. A nematic liquid crystal is found to have many different viscosity coefficients known as *Leslie coefficients*. There are five independent Leslie coefficients all with the dimensions of viscosity. Their magnitude is comparable to each other, typically in the range of 10^{-2} to 10^{-1} poise [1]. Unlike isotropic liquids, liquid crystals respond to applied mechanical

torques and stresses. The elastic deformation on liquid crystals due to external torques can be resolved into three basic deformations called splay, twist and bend. The associated elastic constants are known as Frank's curvature elastic constants and denoted as K_{11}, K_{22} and K_{33} respectively [1, 2]. In Fig. 1.7 we have shown three basic elastic distortions in a nematic liquid crystal. These elastic constants have units of energy/length and their order of magnitude is generally in the range $10^{-6} - 10^{-7}$ dynes.

The ratio of viscosity coefficient to the elastic constant of a liquid crystal is an important parameter for display technologies and is known as "Viscoelastic Coefficient". In the second, third and fourth chapter of this thesis we have used dynamic light scattering to measure the twist viscoelastic coefficient of nematic liquid crystals. Here, the laser beam was used as a probe and had no effects on its own. On the other hand, it is well known in the case of liquid crystals, that a strong enough laser beam can result in many interesting nonlinear phenomena. A very strong laser field can also alter the order parameter of a liquid crystalline medium. Also, if the medium is absorbing, the order parameter can change with change in the intensity of laser field. These two effects together can lead to many interesting situations in liquid crystal phase transitions. In the following sections we describe dynamic light scattering and nonlinear optics in general.

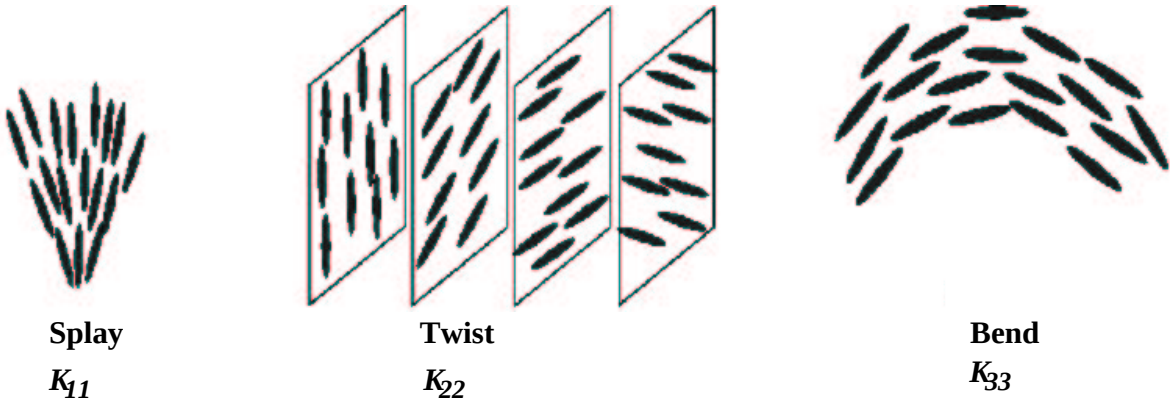

Figure 1.7: Three basic elastic deformations in a nematic liquid crystal.

1.3 Dynamic light scattering

Dynamic light scattering is a powerful tool to probe the dynamics of a given medium. There are always thermal fluctuations in a system at any nonzero temperature and this leads to fluctuations in the refractive index [5]. These refractive index fluctuations are responsible for the scattering of light. When a medium with such refractive index fluctuations is illuminated with a coherent source of light (*i.e.* laser), a fluctuating speckle pattern is formed in the far field. A schematic diagram of basic arrangement of a light scattering setup is shown in Fig. 1.8. A linearly polarized (in a direction **i**) light beam is scattered by the medium. The scattered light passes through an analyzer which selects a particular polarization **f** before the light enters the detector. We denote the incident wave vector and scattered wave vector of the light beam by $\mathbf{k_i}$ and $\mathbf{k_f}$, respectively. The intersection of main beam and the scattered beam defines the scattering volume involved in the scattering process. The detector senses the fluctuating intensity of the scattered light. By analyzing the intensity fluctuations we can get the information about the dynamics in the scattering volume.

The fluctuations are studied by analyzing the intensity temporal auto correlation function of scattered light. Now, we briefly describe the auto correlation function of fluctuating light intensity at the detector.

1.3.1 Auto correlation function

Dynamic light scattering is used, generally, to find the size and distribution of micron sized particles suspended in a liquid. At a non-zero temperature, these particles undergo Brownian motion. We consider $A(t)$, some property of this system at any time t that depends on position and momentum of particles in the system. Due to the Brownian motion of particles, $A(t)$ also fluctuates randomly about a mean value $\langle A \rangle$. A plot of $A(t)$ as a function of time looks like a random signal. The average value of A *i.e.* the bulk property of the system in the equilibrium state is given by:

$$\langle A \rangle = \lim_{T_t \to \infty} \frac{1}{T_t} \int_0^{T_t} A(t) dt \tag{1.5}$$

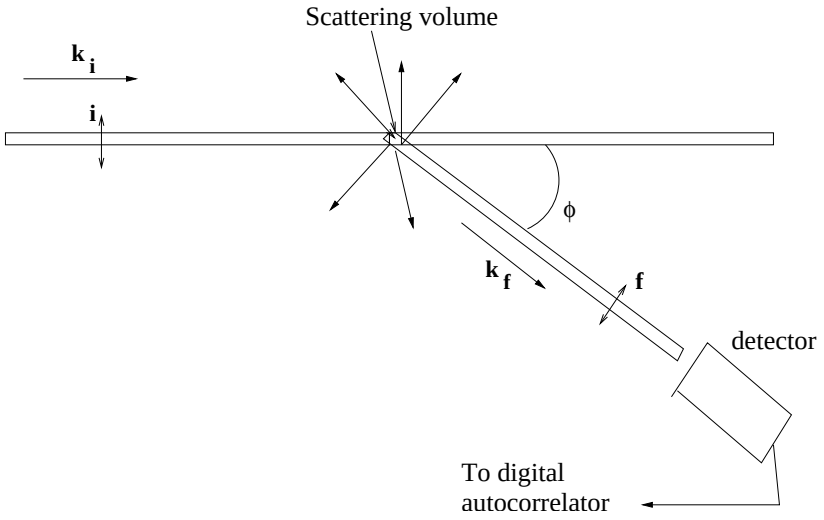

Figure 1.8: The basic arrangement of a light scattering setup. The incident and scattered wave vectors are denoted by $\mathbf{k_i}$ and $\mathbf{k_f}$, respectively and ϕ is the scattering angle.

Here, T_t is the total time over which $A(t)$ is measured. The average value of A can be taken to be zero. Auto correlation function (ACF) is a measure of the correlation between two values of parameter A at two different times t and $t + \tau$. Here, τ is called the delay time. The auto correlation function is written as:

$$\langle A(0)A(t)\rangle = \lim_{T_t\to\infty} \frac{1}{T_t} \int_0^{T_t} A(t)A(t+\tau)dt \tag{1.6}$$

The above discussion pertains to a continuous temporal correlation. In practice, a digital correlator is used to perform discrete time auto correlation. The time axis is divided into discrete equally spaced intervals Δt such that $t = i\Delta t$ where, $i = 1, 2, 3, ...$ The parameter $A(t)$ is sampled at these intervals. The delay time (τ) is expressed as $\tau = mt$ (m being an integer) and is introduced by correlator between two samples of $A(t)$. The total integration time is $M\Delta t$ where M is the total number of samples. The variation of $A(t)$ is shown in Fig. 1.9. The sampling time is chosen to be small enough so that the sampled $A(t)$ is almost same as the continuous $A(t)$. The average value of A in the sampled data is then given by:

$$\langle A\rangle \equiv \frac{1}{M} \lim_{M\to\infty} \sum_{i=1}^{M} A_i \tag{1.7}$$

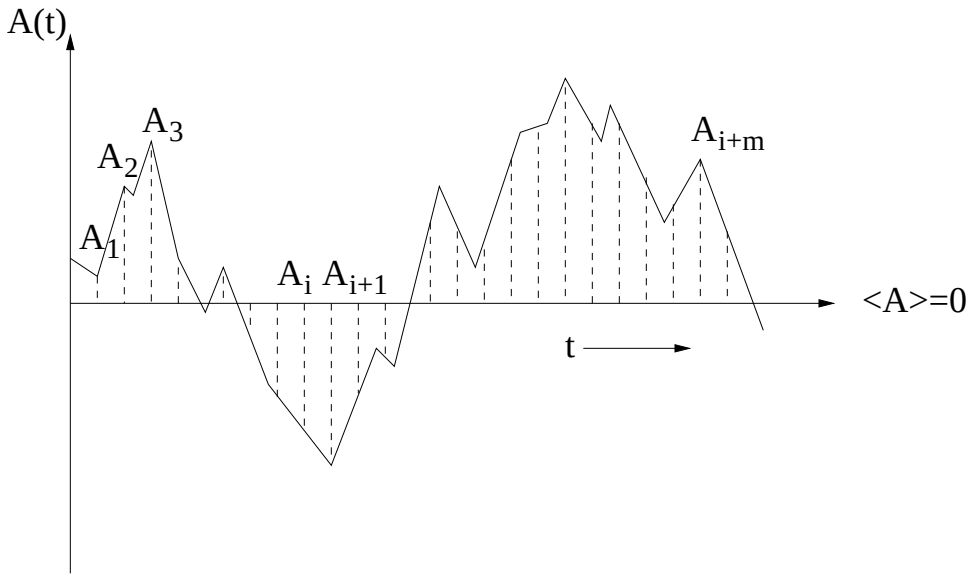

Figure 1.9: The property $A(t)$ fluctuates in time as the particles undergo Brownian motion in the liquid. The time axis is divided into discrete intervals, Δt. Sampling time is chosen small enough so that the sampled data represent the continuous data.

The discrete auto correlation function is given by:

$$\langle A(0)A(\tau)\rangle \equiv \frac{1}{M-m}\lim_{M\to\infty}\sum_{i=1}^{M} A_i A_{i+m} \tag{1.8}$$

For the zero delay, *i.e.* $m = 0$, all the terms in the above equation have positive values, but for $m \neq 0$, the summation will have both positive and negative terms. As $m \to M$, in case of a random signal, we expect ACF to decay to zero at longer times. To start with, at $\tau = 0$ an ACF has the value:

$$\langle A(0)A(\tau)\rangle = \langle A^2\rangle \tag{1.9}$$

But as $\tau \to \infty$, $A(0)$ and $A(\tau)$ become more and more uncorrelated and hence,

$$\langle A(0)A(\tau)\rangle \equiv \langle A(0)\rangle\langle A(\tau)\rangle = \langle A\rangle^2 \tag{1.10}$$

Hence, the variation of $A(t)$ for the suspension of spherical particles in a liquid, seems like a random signal as shown in Fig. 1.10(a) and the ACF decays with delay time from $\langle A^2\rangle$ to $\langle A\rangle^2$ as shown in Fig. 1.10(b). If $A(t)$ is the intensity of scattered light from the uniform monodisperse spherical particles suspended in liquid and undergoing Brownian motion, the

ACF decays like a single exponential.

$$\langle A(0)A(\tau)\rangle = \langle A\rangle^2 + \left(\langle A^2\rangle - \langle A\rangle^2\right)\exp\frac{-\tau}{\tau_r} \tag{1.11}$$

Here, τ_r is the *relaxation time* and this gives the information about how long the intensity of scattered light is correlated with itself. The relaxation time is related to the hydrodynamic radius[3] of particles by Stokes-Einstein relation.

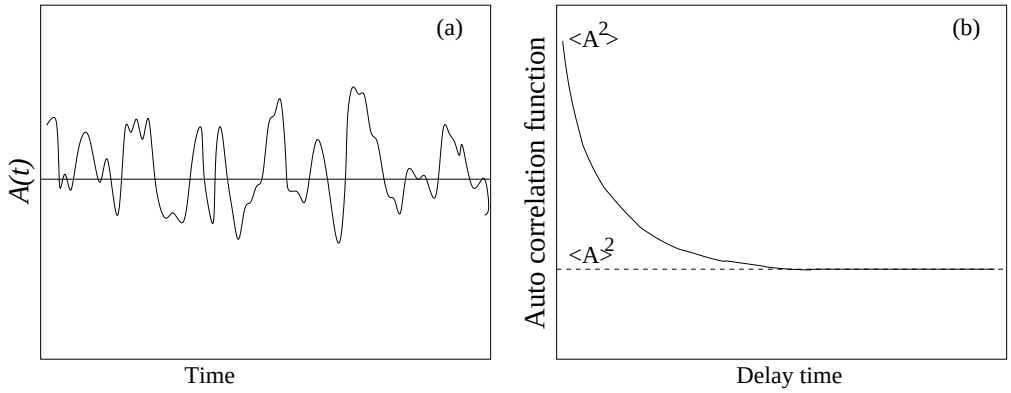

Figure 1.10: (a) The variation of $A(t)$ from a suspension of spherical particles in a liquid as a function of time. (b) The time averaged auto correlation function of $A(t)$. The proerty $A(t)$ can be the intensity of light scattered from the suspension.

The detector we use in DLS experiments, senses the intensity of the scattered light. In all DLS experiments, we get the intensity auto correlation function from which we deduce the relaxation time. This relaxation time is the most important quantity which is of concern to us in all DLS experiments. We now discuss the relation between electric field and experimentally measured intensity correlation function.

In homodyne light scattering experiments, where only the light scattered from the sample reaches the detector, the scattered electric field ($E(t)$) is proportional to the change in dielectric constant of the medium. The intensity auto correlation function is related to field correlation function by the well known Siegert's relation as given by [6]:

$$\langle I(0)I(\tau)\rangle = \langle I^2\rangle + |\langle E(0)E^*(\tau)\rangle|^2 \tag{1.12}$$

[3]DLS measures the radius of spheres that diffuses in the medium. In practice, macromolecules in solution may be non spherical. So, the radius calculated from the diffusional properties of the particle is indicative of apparent size of the dynamic hydrated particle and is called as hydrodynamic radius.

The electric field correlation function is denoted as $g_1(\tau)$ and intensity auto correlation function is denoted as $g_2(\tau)$.

$$g_1(\tau) = \frac{\langle E(0)E^*(\tau)\rangle}{\langle I\rangle} \tag{1.13}$$

$$g_2(\tau) = \frac{\langle I(0)I(\tau)\rangle}{\langle I^2\rangle} \tag{1.14}$$

Siegert's relation can also be written as follows [6]:

$$g_2(\tau) = 1 + \beta|g_1(\tau)|^2 \tag{1.15}$$

where, β is the coherence factor which depends on the effective area of the detector. The value of β can be extracted directly from the correlogram by the intercept of normalized correlation function on y-axis. Its maximum value can be 1 which shows a high signal to noise ratio. In an experiment, to achieve smaller detector area[4] one has to put a small pinhole in front of the detector. But, if the total scattering intensity is small, then a smaller pinhole will lead to smaller counts and hence poor signal. So, a compromise between the pinhole size and the count rate is made during the experiment.

In order to extract the material property of the sample, the auto correlation function thus obtained has to be analyzed. In the next section, we describe some of the important methods to analyze the intensity correlation function.

1.3.2 Analysis of correlation function

We now discuss some of the commonly used techniques for analyzing DLS data. In general, there are more than one relaxation processes in a given sample which leads to many independent relaxation times. The general form of correlation function is given by [7]:

$$g_2(\tau) = A + \left[\sum_{i=1}^{N} B_i \exp[-\Gamma_i\tau]\right]^2 \tag{1.16}$$

where, A is a constant baseline, B_i is the relative amplitude of ith decay process with decay rate Γ_i.

[4]For a good experimental measurement, detector area should be equal to coherence area.

Single or double exponential analysis:

This is the simplest method of analysis, but is applicable only when one has the apriori knowledge of the system [5, 7]. If there is only one decay process[5] in the system, then the auto correlation function can be easily expressed by a single exponential function with a characteristic decay time τ_r:

$$g_2(\tau) = A + B\exp(-2\tau/\tau_r) \tag{1.17}$$

Here, the factor 2 indicates the homodyne configuration and A is constant baseline.

In order to characterize two widely separated relaxation processes (such as in the case of a mixture of mono disperse uniform particles of two different sizes), one can represent the correlation function as a sum of two exponential functions:

$$g_2(\tau) = A + [B\exp(-\tau/\tau_1) + C\exp(-\tau/\tau_2)]^2 \tag{1.18}$$

This method is useful when two relaxation times τ_1 and τ_2 are well separated. If these two relaxation times have comparable values, then nonlinear least squares fit to determine the five adjustable parameters may not converge.

Cumulant analysis:

This is a very important method to analyze the data of a polydisperse system. It was first proposed by Koppel in 1972 [8]. This is based on series expansion of exponential functions. The generalized form of field correlation function $g_1(\tau)$:

$$g_1(\tau) = \sum_{i=1}^{N} a_i \exp(-\Gamma_i \tau) \tag{1.19}$$

This in the limit of $\tau \to 0$ is given as a power series in τ:

$$\ln(g_1(\tau)) = A + B\tau + C\tau^2 \tag{1.20}$$

When this is plotted against τ, the intercept on y-axis is A which is a measure of the coherence factor β as discussed earlier. B is related to the average particle size and the coefficient

[5] A system of mono disperse uniform spherical particles suspended in a liquid or a well aligned liquid crystal in a properly chosen geometry will have only one decay process.

C is the measure of the deviation from linearity and is related to the polydispersity of the system.

CONTIN and DISCRETE analysis:

CONTIN and DISRETE [9, 10] are packaged programs which were made available on request. CONTIN assumes a continuous distribution of amplitudes while DISCRETE intercepts correlation function in terms of discrete decay functions. CONTIN is composed of a fixed core of 53 subprogram. It is not a user interactive program.

Apart from these methods, there are also few more methods[6] used in special cases to analyze DLS data. We have used single exponential method to analyze our data because we know that in a properly chosen geometry in a well aligned nematic liquid crystal we get only one decay process. In addition to this, we have calibrated our experimental setup using standard uniform spherical particles. For analyzing the data from these particles we used cumulant method via a commercial software DYNALS (Alango Ltd.). In the next section, we discuss the light scattering from nematic liquid crystals.

1.3.3 Dynamic light scattering from nematics

Nematic liquid crystals are turbid in appearance and strongly scatter light. Earlier this strong scattering of light was attributed to small (micron size) optically anisotropic objects, scattering light in all directions [1]. This was known as *swarm theory*. But, later Chatelain [11] showed that the scattering was intense and scattered light was depolarized. Then, de Gennes [1] theoretically showed that the reason for the strong light scattering by nematic is due to the presence of spontaneous fluctuations of the director. Thermal fluctuations cause the spatial and temporal fluctuations in the director and hence, the dielectric tensor also fluctuates. This causes the high scattering of light passing through the liquid crystal. It is worth mentioning here that the usual density fluctuations also can cause the fluctuations in dielectric tensor and result in scattering of light as in the case of usual isotropic liquids. But, such scattering is considerably weaker (a factor of about 10^{-6}) than that arising due to the by di-

[6] Inverse Laplace transform method, Overlay histogram method with exponential sampling.

rector fluctuations [12]. Thus, the dominant scattering of light in case of liquid crystals is due to orientational fluctuations and can be used to obtain the information about the various modes of orientational fluctuations and their dynamics.

In an ideal nematic, all molecules are oriented parallel to $\mathbf{n_0}$. To describe thermal fluctuations in the alignment, a continuum theory can be used in which the detailed order on the molecular scale is ignored and the local director is considered as a function of the position $\mathbf{r}$. Then:

$$\mathbf{n}(\mathbf{r}) = \mathbf{n_0} + \delta\mathbf{n}(\mathbf{r}) \tag{1.21}$$

Here, $\delta\mathbf{n}(\mathbf{r})$ is the deviation of $\mathbf{n}(\mathbf{r})$ from the equilibrium. The orientational order parameter varies in accordance with **n(r)**. The dielectric tensor can be written as,

$$\epsilon_{\alpha\beta}(\mathbf{r}) = \epsilon_\perp \delta_{\alpha\beta} + (\epsilon_\parallel - \epsilon_\perp)\mathbf{n}_\alpha(\mathbf{r})\mathbf{n}_\beta(\mathbf{r}) \tag{1.22}$$

where, $\epsilon_\perp$ and $\epsilon_\parallel$ are the dielectric constants perpendicular and parallel to the optic axis. The dielectric anisotropy ϵ_a is:

$$\epsilon_a = \epsilon_\parallel - \epsilon_\perp \tag{1.23}$$

The fluctuations in dielectric tensor can be expressed as:

$$\delta\epsilon_{\alpha\beta} = \epsilon_a \left(\delta n_\alpha n_{0\beta} + n_{0\alpha}\delta n_\beta\right) \tag{1.24}$$

In nematics, scattered intensity depends on the mean square amplitude of thermal fluctuations in two uncoupled, non propagating eigenmodes represented by δn_1 and δn_2. To evaluate the amplitudes of these two normal modes, we write the nematic free energy (F_N) as given by the following Eqn.:

$$F_N = \frac{K_{11}}{2}(\nabla.\mathbf{n})^2 + \frac{K_{22}}{2}(\mathbf{n}.\nabla\times\mathbf{n})^2 + \frac{K_{33}}{2}(\mathbf{n}\times\nabla\times\mathbf{n})^2 \tag{1.25}$$

Each component of the director fluctuations can be expressed in terms of its Fourier series:

$$\delta n_\alpha(\mathbf{r}) = \Omega^{-1}\sum_{\mathbf{q}} \delta n_\alpha(\mathbf{q}) \exp(-i\mathbf{q}.\mathbf{r}) \tag{1.26}$$

where, **q** is the wave vector of director fluctuations and Ω is the sample volume. Using this and applying equipartition theorem, we obtain the mean square amplitude of the two normal modes for the wave vector **q**:

$$\langle|\delta n_1(\mathbf{q})|^2\rangle = \frac{k_B T_A}{K_{11} q_\perp^2 + K_{33} q_\parallel^2} \tag{1.27}$$

$$\langle|\delta n_2(\mathbf{q})|^2\rangle = \frac{k_B T_A}{K_{22} q_\perp^2 + K_{33} q_\parallel^2} \tag{1.28}$$

Here, k_B is the Boltzmann constant, T_A is the absolute temperature and $q_\parallel$ and $q_\perp$ are the components of wave vector parallel and perpendicular to the director, respectively. It is clear from the Eqn. 1.27 and 1.28 that the first mode is a combination of bend and splay while the second mode is a combination of bend and twist distortions in the director. By comparing the elastic free energy to viscous free energy, we get the relaxation frequencies for two modes:

$$\Gamma_1(\mathbf{q}) = \frac{K_{11} q_\perp^2 + K_{33} q_\parallel^2}{\eta_1(\mathbf{q})} \tag{1.29}$$

$$\Gamma_2(\mathbf{q}) = \frac{K_{22} q_\perp^2 + K_{33} q_\parallel^2}{\eta_2(\mathbf{q})} \tag{1.30}$$

where η_1 and η_2 are the viscosities for mode 1 and mode 2 respectively. η_1 and η_2 are related to Miesowicz viscosities (η_a, η_b, η_c), Leslie coefficients (α_1,α_2, α_3, α_4, α_5) and twist viscosity γ_1 [12]. Individual viscoelastic coefficient can be studied by choosing appropriate direction of scattering wave vector (**q**) and polarization of incident and scattered light with respect to the optic axis. In Fig. 1.11 we have shown specially chosen experimental geometries. For example, the geometry of Fig. 1.11(a) leads to single splay mode relaxation rate:

$$\Gamma_{splay}(\mathbf{q}) = \frac{K_{11} q^2}{\gamma_1 - \alpha_3^2/\eta_b} \tag{1.31}$$

the geometry in Fig. 1.11(b) leads to a single twist mode relaxation rate:

$$\Gamma_{twist}(\mathbf{q}) = \frac{K_{22} q^2}{\eta_2} \tag{1.32}$$

and the geometry in Fig. 1.11(c) leads to a single bend mode relaxation rate:

$$\Gamma_{bend}(\mathbf{q}) = \frac{K_{33} q^2}{\gamma_1 - \alpha_2^2/\eta_c} \tag{1.33}$$

Thus, in nematic liquid crystals, DLS measurement in the appropriate geometry can yield the ratio between the relevant Frank elastic constant and a combination of viscosity coefficients [13, 14]. We have used this theory to measure the twist viscoelastic coefficient of

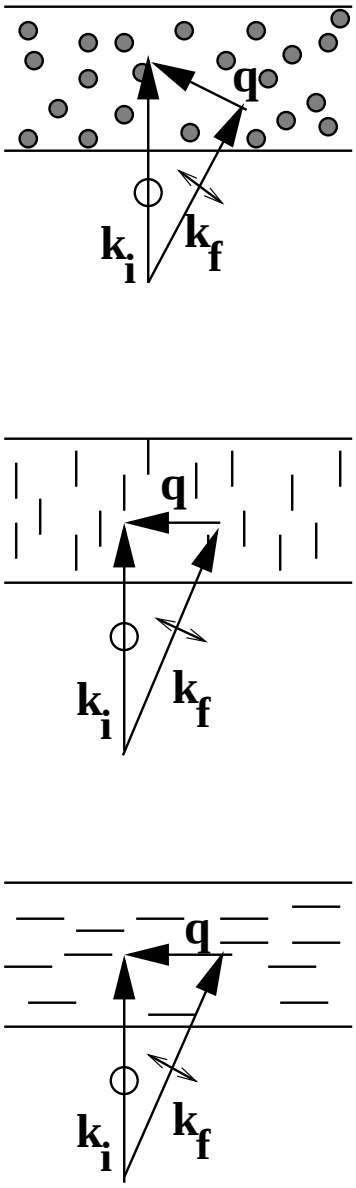

Figure 1.11: Three different scattering geometries for trapping individual viscoelastic modes. (a) leads to single splay mode relaxation (b) leads to single twist mode relaxation and (c) leads to single bend mode relaxation of the director in a nematic liquid crystal [12].

nematic liquid crystals. In these experiments, the laser beam is not intense enough to induce any effects on its own. But, an intense laser beam can induce many interesting effects on liquid crystals. We describe some of these effects in the next section.

1.4 Nonlinear optics

Nonlinear optics is the branch of optics which describes the behavior of light in a nonlinear media. A nonlinear medium is one in which polarization nonlinearly responds to the electric field of light [15]. Nonlinear optical effects have been observed since 19th century in the form of Pockel's effect and Kerr effect. Later in 1960 the invention of laser gave a new dimension to nonlinear optics. A very high electric field associated with laser beam gives rise to many new phenomena like second harmonic generation, four wave mixing and self phase modulation. In case of usual linear media, the induced polarization (**P**) is linearly related to the electric field (**E**) of the light beam.

$$\mathbf{P} = \chi \mathbf{E} \tag{1.34}$$

Here, χ is a second rank tensor and it is called as the susceptibility of the medium. But, the above equation is not strictly true. In all materials the polarization can be expanded in a power series in electric field.

$$\mathbf{P} = \chi^{(1)}\mathbf{E} + \chi^{(2)}\mathbf{EE} + \chi^{(3)}\mathbf{EEE} + ... \tag{1.35}$$

where $\chi^{(2)}$, $\chi^{(3)}$.... are the second and third order nonlinear susceptibilities. Usually, it is found that the order of magnitude of $\chi^{(2)}$ is much less than that of $\chi^{(1)}$. So, in practice, at lower light intensities the linear term is dominant and hence the nonlinear effects do not play a significant role at normal light intensities. We now briefly discuss some of the nonlinear effects found in usual nonlinear medium.

Nonlinear optical effects:

Second harmonic generation (SHG) is well studied nonlinear optical effect since it was the first to be discovered. It is widely used to obtain new coherent waves from the laser sources to be used in a wide range of experiments and applications. This effect corresponds to the generation of a new wave at a frequency twice to that of the input beam. In the nonlinear medium, for the incident beam of frequency ω we get the fundamental at frequency ω and its second harmonic at frequency 2ω. SHG corresponds to second order nonlinearity and this is

not found in symmetric and isotropic crystals because in these crystals, due to symmetry, the second order nonlinear susceptibility is zero.

Another important nonlinear effect is the wave mixing, where three light beams at frequencies ω_1, ω_2 and ω_3 interact in a nonlinear medium and give rise to a fourth wave of frequency $\omega_4 = \omega_1 + \omega_2 - \omega_3$ or $\omega_4 = \omega_1 - \omega_2 + \omega_3$ or other possible combinations. While the energy conservation is always fulfilled, the nonlinear effects can be observed only when the momentum conservation is realized. Momentum conservation is also known as *phase matching* condition. Sometimes it occurs spontaneously otherwise one must find the right experimental configurations to realize this condition.

Sometimes nonlinear optical effects occur without the generation of new waves having different frequencies or wave vectors, from the one which is incident on the nonlinear medium. But, the nonlinear behavior is shown by the self induced change in the propagation characteristic of the single wave traveling through the medium. This is the manifestation of third order nonlinearity. The refractive index is found to be a function of the incident light intensity. This intensity dependent refractive index can lead to strong effects on the propagation of laser beams, leading to self focusing or self divergence. If the incident light beam has an intensity profile in the transverse direction, then it can give rise to an intensity dependent refractive index which transforms the medium to a lens, effectively. If the central part of the beam having higher intensity, experiences the higher refractive index then, as a consequence the speed of the wave is slower at the center compared to that at the edge of the beam. In this case the original wave front is distorted and the beam appears focused by itself. In general, the refractive index n is written as:

$$n = n_0 + \Delta n I \tag{1.36}$$

where, n_0 is the intrinsic refractive, Δn is the change in refractive index and I is the intensity of light. The nonlinear optical coefficient (n_2) is defined as:

$$n_2 = \Delta n / I \tag{1.37}$$

For $n_2 > 0$ we get self focusing and for $n_2 < 0$ we get self divergence.

1.4.1 Nonlinear optics in liquid crystals

Liquid crystals are known to have very high nonlinear optical effects. In case of usual nonlinear media, mainly the electronic processes are responsible for various nonlinear optical effects. But, in case of liquid crystals the mechanisms which lead to a high nonlinear optical coefficients are very different. We discuss a few of them here.

1.4.1.1 Light induced director reorientation

The first report of giant optical nonlinearity in nematic liquid crystal was reported in 1980 [16, 17]. A moderate power He-Ne laser beam was used to observe self focusing in a homogeneously aligned liquid crystal sample with a positive dielectric anisotropy ($\epsilon_{\parallel} > \epsilon_{\perp}$). The nonlinear dielectric permittivity measured was 0.07 esu compared to 1.2×10^{-10} esu in a so called strong nonlinear medium CS_2. The mechanism involved in this case is "director reorientation" due to the electric field of the laser beam [18]. It is well known that a low frequency electric field can be used to reorient the director of a nematic liquid crystal[7] along the direction of applied field. In a similar fashion, the director reorientation can take place by the application of a high frequency optical field. The earlier experiments were carried out using a planar nematic cell with a linearly polarized light. The laser beam is incident on the sample at an angle different from zero as shown in Fig. 1.12. The light was focused at a point before it entered the cell in order to have a diverging beam onto the sample. Under these conditions it is easy to see a remarkable decrease in the beam diameter in the far field by increasing the light intensity. This is the direct consequence of self focusing inside the liquid crystal cell. In a beam having Gaussian intensity distribution[8], the refractive index seen by the beam will be maximum at the center. This leads to a reorientation of director towards the light polarization direction. This results in an increase in the refractive index which approaches to its maximum value n_e at the center. It decreases to n_{eff} with increasing distance from the center of wavefront where the intensity also decreases. The value of n_{eff}

[7] One should note that this kind of reorientation takes place only for nematics having positive dielectric anisotropy. For nematics having negative dielectric anisotropy, the molecules align in a plane perpendicular to the applied field.

[8] almost all the lasers have a Gaussian intensity profile along the wavefront.

is given by:

$$n_{eff} = \frac{n_e n_o}{\left(n_e^2 \cos^2 \xi + n_o^2 \sin^2 \xi\right)^{1/2}} \tag{1.38}$$

here, ξ is the angle between the direction of light and the director.

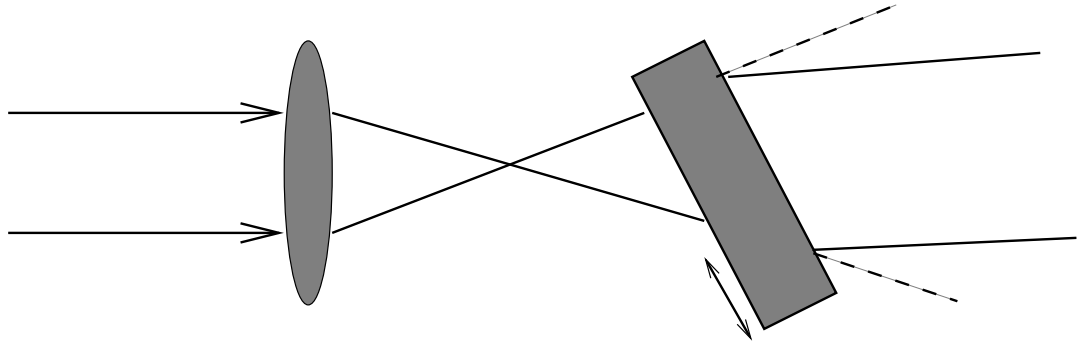

Figure 1.12: The experimental geometry to observe the self focusing in a homogeneously aligned nematic cell.

In an isotropic phase of rod like molecules also one can have laser induced molecular reorientation. An intense laser field can force the anisotropic molecules to align themselves in the direction of the optical field through the dipolar interaction. This process is often termed as laser induced ordering and such a phase is known as paranematic phase. The nonlinear optical coefficient due to the individual molecular ordering in isotropic phase is directly proportional to the laser induced order parameter [18].

It has been observed in recent studies [19] that, in addition to the director reorientation due to the dielectric anisotropy, some absorbing dye doped nematic liquid crystals show very high nonlinear optical effects. The excited dye molecules exert an intermolecular torque on the liquid crystal molecules which could be stronger than the optical torque. This was observed with some special class of dye molecules (anthraquinone dyes) which on photo excitation further enhance such torque effects.

The director reorientation can also lead to high nonlinear effects in other liquid crystal phases like smectics and cholesterics. The basic mechanism of laser induced molecular reorientation in smectic phases is similar to that occurring in nematic phase. The main difference

lies in the magnitude of the various physical parameters that distinguish the smectic from the nematic phase. The tendency of smectics to have a layered structure imposes a restriction on reorientation of molecules by an external field. The possibility of laser induced director reorientation was first discussed by Tabiryan *et. al.* [20]. For smectic A liquid crystals it is clear that the director reorientation will involve a change in layer spacing and such a distortion will require an enormous energy. Therefore, this is not observable under finite field strength. But, in smectic C liquid crystals, it is possible to reorient the azimuthal component of the director. This requires only the rotation of the director about the layer normal and hence does not change the layer spacing. The optical nonlinearity associated with such a reorientation process is comparable to that in the nematic phase.

There are a few more mechanisms in liquid crystals other than director reorientation which lead to a high nonlinear optical effect. Thermal nonlinearities are also very high in case of liquid crystals. We briefly describe the thermal effects in liquid crystals in the next section.

1.4.1.2 Thermal effects

The absorption of light by a liquid crystal[9] can increase the temperature of the medium. As a consequence, the physical properties of liquid crystal changes and this affects the propagation of the incident light beam. The refractive indices of a liquid crystal are temperature dependent and hence most important to be considered here. The change in refractive index of a liquid crystal, due to the absorption of the light beam, is known as "Thermal Indexing". Generally, the extraordinary refractive index decreases and ordinary refractive index increases as a function of temperature. Thermal gradient in refractive indices are important to understand the thermal nonlinear behavior of a liquid crystal. It is found that in case of liquid crystals, this thermal gradient is at least one order of magnitude higher than that in usual liquids. These gradients are strongly enhanced near the liquid crystal to the isotropic phase transition temperature. These features are very interesting from the point of view of nonlin-

[9]It may be caused either by the liquid crystal itself or by small impurities present in the medium.

ear optics and they are responsible for the unusually high thermal nonlinearity. Apart from this, liquid crystals can be doped easily with some absorbing dyes, leading to an increase in absorption which produces remarkable heating at low laser intensities. In this way, the thermal nonlinearities become very large. The refractive index gradients for extraordinary and ordinary refractive indices are given by [18]:

$$\frac{dn_e}{dT} = \frac{1}{2n_e}\frac{d\epsilon_{\|}}{dT} \tag{1.39}$$

$$\frac{dn_o}{dT} = \frac{1}{2n_o}\frac{d\epsilon_{\perp}}{dT} \tag{1.40}$$

here, n_e and n_o are the extraordinary and ordinary refractive indices, respectively. In practice thermal gradient in n_o is positive and in n_e is negative. This is due to the fact that as we approach liquid crystal to isotropic transition, both refractive indices approach the isotropic value (n_{iso}) which is an intermediate value between n_e and n_o. In the case of thermal indexing, we have nonlinear behavior in ordinary wave with a different sign with respect to the one in the extraordinary wave. As a consequence, we always have self focusing for extraordinary wave and self divergence for ordinary wave.

In a cholesteric liquid crystal, when the pitch is small compared to the wavelength of light, the base states are right and left circular waves. The refractive indices for these waves can be a function of laser intensity leading to a large nonlinear optical coefficient.

Also, in liquid crystals there is an interesting temperature dependence of orientational order parameter. Hence, it is often difficult to separate thermal effects from the ordering effects. There is also a possibility of light induced phase transitions, for example, from the nematic to isotropic with a jump in the values of refractive index and other material parameters [18]. This by itself can lead to strong nonlinear optical behavior. In the same situation for large laser beam intensity the order parameter of the system can change. In such cases, the electric field of the laser beam can transform an isotropic phase to a paranematic phase. Then, there will be a compromise between the laser absorption and electric field of the laser beam.

In this thesis, we describe the dynamic light scattering (DLS) studies and nonlinear opti-

cal properties of liquid crystals. We studied the viscoelastic coefficient of lyotropic discotic nematic liquid crystals by employing DLS. The system studied was Cesium perfluorooctanoate (CSPFO), which forms disk like micelles over a range of concentration in water. We find that the twist viscoelastic coefficient increases as we increase the temperature in the nematic phase. It is also a sensitive function of the concentration of CSPFO in water. We have doped a polymer in the CSPFO water system and find that the twist viscoelastic coefficient decreases in the nematic phase as the concentration of polymer increases. We have doped a salt in the CSPFO water system and studied the viscoelastic modes in the nematic phase. We have investigated the viscoelastic coefficients of homologous series of novel thiol terminated alkoxy-cyanobiphenyl liquid crystals. We find that the twist viscoelastic coefficient is 3-4 times smaller compared to that in alkoxy-cyanobiphenyl liquid crystals.

We have theoretically worked out the thermo-nonlinear optical coefficient of a cholesteric liquid crystal. We find that the nonlinear optical coefficient can be as high as $10^{-4}\ cm^2/W$ in some cases. When the intensity is too high, the effect of laser electric field becomes significant. We have also considered such situation in weakly absorbing liquid crystals and found many interesting results. The effects of linear dichroism and laser electric field were studied theoretically using the Landau deGennes theory.

Bibliography

[1] De Gennes P.G. and Prost J., *The Physics of Liquid Crystals*, Oxford University Press, UK, 2001.

[2] Collings P.J. and Hird M., *Introduction to Liquid Crystals: Chemistry and Physics*, Taylor and Francis, London, UK, 1997.

[3] Gelbart W.M., Ben-Shaul A. and Roux D., *Micelles, membranes, micro-emulsions, and monolayers*, Springer Verlag, New York, 1994.

[4] Demus D. and Richter L., *Textures of Liquid Crystals*, Verlag-Chemie, Weinheim, 1978.

[5] Berne B.J. and Pecora R., *Dynamic Light Scattering*, Wiley-Interscience publication, Toranto, 1976.

[6] Lemieux P.A. and Durian D.J., *J. Opt. Soc. Am. A* **16**, pp. 1651, (1999).

[7] Schmitz K.S., *An Introduction to Dynamic Light Scattering by Macromolecules*, Academic Press Inc., San Diego, 1990.

[8] Koppel D.E., *J. Chem. Phys.*, **57** pp. 4814 (1972).

[9] Provincher S.W., *Comp. Phys.*, **27** pp. 213 (1982).

[10] Provincher S.W., *Comp. Phys.*, **27** pp. 224 (1982).

[11] Chatelain P., *Acta Cristallogr.*, **1** pp. 315 (1948).

[12] Kumar S., *Liquid Crystals: Experimental study of Physical Properties and Phase Transitions*, Cambridge University Press, UK, 2001.

[13] Group d'Etude des Cristaux Liquides, *J Chem. Phys.*, **51** pp. 816 (1969).

[14] Fellner H., Frnaklin W. and Christensen S., *Phys. Rev. A*, **11** pp. 1440 (1975).

[15] Yariv A., *Optical Electronics*, Harcourt Brace, Philadelphia, 1971.

[16] Zel'dovich B.Ya., Pilipetskii N.F., Sukhov A.V. and Tabiryan N.V., *JETP Lett.*, **31** pp. 264 (1980).

[17] Pilipetskii N.F., Sukhov A.V., Tabiryan N.V. and Zel'dovich B.ya., *Opt. Comm.*, **37** pp. 280 (1981).

[18] Simoni F., *Nonlinear Optical Properties of Liquid Crystals and Polymer Dispersed Liquid Crystals* World Scientific Press, Singapore, 1997.

[19] Janossy I., Csillag L. and Lloyd A.D., *Phys. Rev. A*, **44** pp. 8410 (1991).

[20] Tabiryan N.V. and Zel'dovich B.Ya., *Mol. Cryst. Liq. Cryst.*, **62** pp. 637; **69**, pp. 19; **69**, pp. 31 (1981).